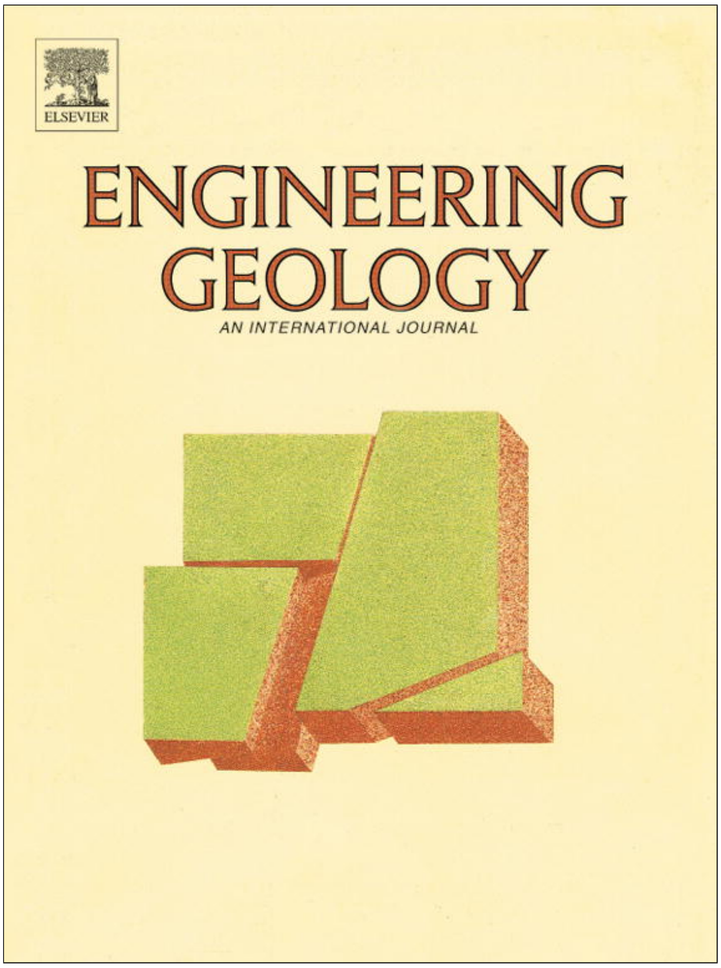
ELSEVIER
ENGINEERING
GEOLOGY
AN INTERNATIONAL JOURNAL

Engineering Geology 153 (2013) 105–113

Contents lists available at SciVerse ScienceDirect

Engineering Geology

journal homepage: www.elsevier.com/locate/enggeo

# Combined roles of saturated permeability and rainfall characteristics on surficial failure of homogeneous soil slope

Wei Chao Li [a,b,*], Lee Min Lee [c], Hong Cai [a,b], Hong Jie Li [d], F.C. Dai [e], Ming Long Wang [f]

[a] State Key Laboratory of Simulation and Regulation of Water Cycle in River Basin, Beijing 100048, China
[b] China Institute of Water Resources and Hydropower Research, Beijing 100048, China
[c] Department of Civil Engineering, Faculty of Engineering and Science, Universiti Tunku Abdul Rahman, 53300 Kuala Lumpur, Malaysia
[d] Institute of Mine Safety Technology, China Coal Research Institute, Beijing 100013, China
[e] Institute of Geology and Geophysics, Chinese Academy of Sciences, Beijing 100029, China
[f] Center for Assessment and Development of Real Estate, Shenzhen 518034, China

ARTICLE INFO

*Article history:*
Received 24 May 2012
Received in revised form 21 November 2012
Accepted 24 November 2012
Available online 19 December 2012

*Keywords:*
Rainfall infiltration
Numerical simulation
Matric suction
Soil permeability
Surficial failure

ABSTRACT

Both rainfall characteristics (rainfall intensity and duration) and saturated permeability of soil may influence the type and mechanism of surficial slope failures. In general, the failures can be initiated by two mechanisms, i.e. loss of matric suction through propagation of wetting front, and rise of water table. Up to date, there are still no clear indicators to identify the dominant parameters that control the type of failure for these shallow landslides. This paper investigates the hydraulic responses of soils to the variations of rainfall characteristics and soil permeability through numerical analyses. The results showed that the hydraulic responses to rainfall for a homogeneous infinite slope underlain by an impermeable layer can be divided into two stages: 1) the propagation of wetting front, and 2) the rise of water table. Based on these hydraulic responses, the type and mechanism of failures were deduced from the analytical analyses. Both the rainfall characteristics and saturated permeability were found to be predominant in controlling the hydraulic responses of soil, and hence the occurrence time, depth of failure plane, and type of surficial slope failures.



## 1. Introduction

Instability of unsaturated soil slope triggered by rainfall is a common geohazard in many parts of the world (Au, 1998; Dai et al., 1999; Toll, 2001; Guzzeti et al., 2008; Rahardjo et al., 2009; Godt et al., 2012). Both rainfall characteristics (rainfall intensity, $I$ and duration, $t$) and saturated permeability of soil, $k_{sat}$, may influence the type and mechanism of slope failure initiations (Pradel and Raad, 1993; Lee et al., 2009). In general, the long duration and moderate intensity rainfall is responsible for deep-seated failures, while the short duration and high intensity rainfall triggers shallow failures (Keefer et al., 1987; Wieczorek, 1987; Iverson, 2000; Leroueil, 2001; Aleotti, 2004). With respect to the saturated permeability of soil, the deep-seated failures normally occur in the soils of low saturated permeability, while the shallow failures are typical for the soil slopes with high saturated permeability (Cho and Lee, 2001).

Numerous researchers have attempted to quantify the combined effect of saturated permeability of soil and rainfall characteristics on the rainfall infiltration, suction distributions, and hence slope instability. Mein and Larson (1973) developed an infiltration model known as Mein–Larson model which suggested that the rainfall infiltration into a soil mass is governed by the infiltration capacity of the soil. At the start of a rainfall event when the near-surface soil is in the unsaturated state with high matric suction, the infiltration capacity is higher than the saturated permeability of the soil. As the result, runoff may not occur even if the rainfall intensity is higher than the saturated permeability of soil (i.e. $I > k_{sat}$). However, as the rainfall continues to saturate the near-surface soil, the infiltration capacity will be reduced to a minimum value equals to the saturated permeability. Beyond this point, the rainfall infiltration is controlled by the saturated permeability of soil. Kasim et al. (1998) performed a series of numerical simulations to investigate the influence of hydraulic properties of soil on the pore-water pressure distributions. They concluded that the steady state pore-water pressure was governed by the ratio of rainfall intensity to saturated permeability (i.e., $I/k_{sat}$) and the air-entry value of soil. Their finding was supported by Ng et al. (1999) who extended the research works by considering more parameters such as soil water characteristic curve, initial groundwater table, the presence of impeding layer etc. Lee et al. (2009) investigated the hydraulic responses of four typical types of soils under extreme rainfall conditions. They concluded that the ratio of rainfall intensity to soil saturated permeability (i.e., $I/k_{sat}$) plays an important role in determining the critical rainfall pattern for a soil slope. From the foregoing, it can be concluded that most of the previous researches have focused on the effects of rainfall characteristic and saturated permeability on

* Corresponding author at: Department of Geotechnical Engineering, China Institute of Water Resources and Hydropower Research, Beijing 100048, China.
*E-mail address:* liwc@iwhr.com (W.C. Li).

0013-7952/$ – see front matter © 2012 Elsevier B.V. All rights reserved.
http://dx.doi.org/10.1016/j.enggeo.2012.11.017

the rainfall infiltration and suction distribution in unsaturated soil. Very few studies have addressed their roles on the type and mechanism of slope failure initiations.

Previous studies suggested that the rainfall-induced slope failure can generally be initiated by two mechanisms: 1) rainfall infiltration induces a rise of groundwater which exerts seepage force and adds weight to the slope, and eventually triggers the slope failure. (Cho and Lee, 2002; Crosta and Frattini, 2003; Soddu et al., 2003); 2) rainfall results in a propagation of wetting front causing an increase in water content and loss in matric suction, and subsequently leads to slope failure (Ng et al., 2001; Collins and Znidarcic, 2004; Rahardjo et al., 2007). These two mechanisms are responsible for shallow landslides on many occasions, particularly associated to pyroclastic or volcanic rocks as reported by numerous researchers across the world, i.e. Chigira et al. (2002) in northern Japan, Cardinali et al. (2006) in central Italy, De vita et al. (2012) in southern Italy, Apip et al. (2009) in West Java, Indonesia, etc. These slopes are commonly characterized by shallow volcanic deposits (<5 m), underlain by less permeable rocks. Rainwater tends to infiltrate into the volcanic deposits and flow laterally along the interface of the less permeable rocks. The soil would become saturated if rainfall is sufficiently intense, and eventually trigger a landslide. Despite of the fact that studies pertaining to the two failure mechanisms can be found in abundance, the dominant factors that govern the type of failure mechanism are still unclear. The understanding on the type of failure mechanism of slope is essential for anticipating the landslide occurrence.

This paper aims to investigate the combined effect of rainfall characteristics and saturated permeability on the hydraulic responses of soil slope to rainfall infiltration, and hence on the mechanism of slope failure. First, numerical simulations are carried out to assess the hydraulic responses of soil to various rainfall characteristics and soil permeability. Based on the hydraulic responses obtained, the type and mechanism of failures were deduced from the analytical analyses on the factor of safety equations developed from an infinite slope model.

## 2. Surficial slope stability analysis

Rainfall-induced slope failures are generally shallow and the failure planes are commonly parallel to the slope surface. For this reason, the surficial stability of slope is often evaluated using a single layered infinite slope model (Skempton and DeLory, 1957; Cho and Lee, 2002; Lu and Godt, 2008; Godt et al., 2009).

Fig. 1 shows a section of a typical infinite slope model (Cho and Lee, 2002). The factor of safety (FOS) of the slope is defined by the ratio of resistance force (quantified by the shear strength of soil) to the mobilized force. The resistance force or shear strength of soil computed from the conventional Mohr–Coulomb failure criterion and effective stress concept (Terzaghi, 1936) is expressed as:

$$\tau_f = c' + \sigma' \tan\theta' \tag{1}$$

where

| | |
|---|---|
| $\tau_f$ | shear stress at failure |
| $c'$ | effective cohesion |
| $\sigma'$ | effective normal stress |
| $\phi'$ | effective friction angle |

Based on the Mohr–Coulomb failure criterion in Eq. (1) and the limit equilibrium approach, the factor of safety (FOS) of the infinite slope shown in Fig. 1 can be expressed as:

$$\mathrm{FOS} = \frac{c' + \sigma' \tan\theta'}{W \sin\alpha \cos\alpha} \tag{2}$$

where $\alpha$ is the slope angle and $W$ is the weight of the soil slice. To extend the effective stress concept to unsaturated soil mechanics, several

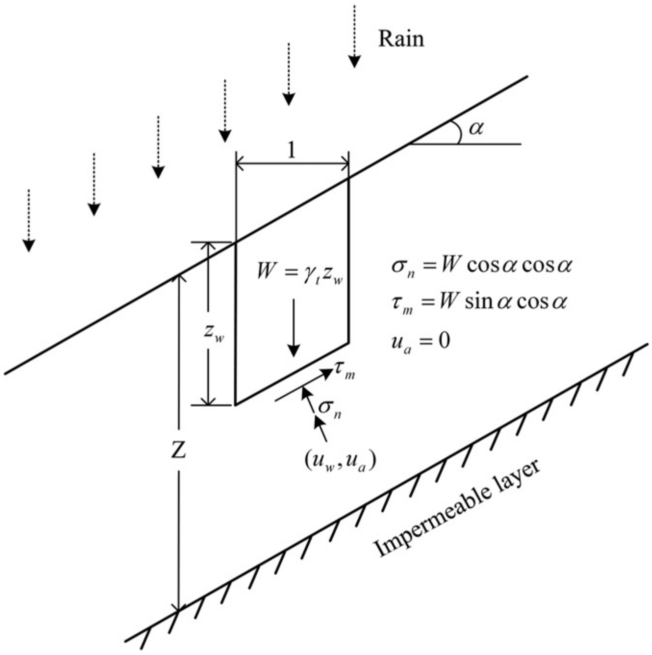


**Fig. 1.** Surficial stability analysis of infinite unsaturated soil slope (reproduced from Cho and Lee, 2002).

functional relations between the effective stress and matric suction have been proposed by numerous researchers (Bishop, 1959; Aitchison, 1960; Jennings and Burland, 1962; Fredlund et al., 1978). Recently, a unified effective stress under both saturated and unsaturated conditions has been suggested by Lu and Likos (2006) and Lu and Godt (2008):

$$\sigma' = (\sigma_n - u_a) - \sigma^s \tag{3}$$

where $u_a$ is the pore-air pressure which can be conveniently taken as 0 (equal to atmospheric), $\sigma_n$ is the total stress due to self weight of soil, and $\sigma^s$ is defined as the suction stress characteristic curve of soil with a general functional form of (Lu and Godt, 2008):

$$\begin{aligned} \sigma^s &= -\frac{\theta - \theta_r}{\theta_s - \theta_r}(u_a - u_w) = -S_e(u_a - u_w) \\ \sigma^s &= S_e u_w \leq 0 \quad \text{for unsaturated conditions } (u_w < 0) \\ \sigma^s &= u_w \geq 0 \quad \text{for saturated conditions} (u_w \geq 0) \end{aligned} \tag{4}$$

whereby $u_w$ is the pore-water pressure, $\theta$ is the volumetric water content, $\theta_r$ is the residual volumetric water content, $\theta_s$ is the saturated volumetric water content, and $S_e$ is the degree of saturation.

By substituting the modified effective stress (Eq. (3)) into Eq. (2), the unified FOS equation for unsaturated and saturated soils can now be expressed as:

$$\mathrm{FOS} = \frac{c' + [(\sigma_n - u_a) - \sigma^s] \tan\theta'}{W \sin\alpha \cos\alpha} \tag{5}$$

As $W = \gamma_t z_w$, $\sigma_n = \gamma_t z_w \cos^2\alpha$, and $u_a = 0$ at atmospheric (where $z_w$ is the vertical depth of soil slice, $\gamma_t$ is the total unit weight of soil), Eq. (5) can be rewritten as:

$$\mathrm{FOS} = \frac{c' + \left(\gamma_t z_w \cos^2 a - \sigma^s\right) \tan\theta'}{\gamma_t z_w \sin\alpha \cos\alpha} \tag{6}$$

The advantage of using Eq. (6) for assessing stability of unsaturated slope is that the analysis can account for both the reduction in matric suction and development of positive pore water pressure in a continuous

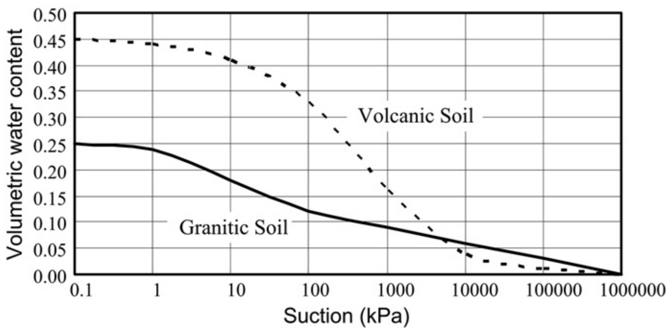


**Fig. 2.** Soil water characteristics curves for the completely weathered granitic material and the completely weathered volcanic material (Sun et al., 1998).

form neglecting the non-linear relation between the shear strength and matric suction as proposed by Fredlund et al. (1978).

For an existing infinite unsaturated slope in which the slope geometry, inclination angle, and shear strength parameters of soil are deemed to be constants, Eq. (6) shows that the stability of slope is dominated by the suction stress characteristic curve of the soil ($\sigma^s$) which in turn is governed by the hydraulic responses of the soil to rainfall, i.e. variation of matric suction and/or development of positive pore water pressure.

## 3. Hydraulic responses of soils to variations of rainfall characteristics and saturated permeability

The hydraulic responses of soil to variations of rainfall characteristics and saturated permeability were evaluated through a series of numerical simulations. A finite element module, Seep/W (GeoSlope International Ltd., 2007), was employed to perform the saturated and unsaturated seepage analysis.

### 3.1. Soil properties

The analyses were carried out to observe the hydraulic responses of two soil slopes in Hong Kong to rainfalls of different constant intensities. The two selected slopes consisted of completely weathered granitic materials at Shouson Hill, and completely weathered volcanic materials at Chai Wan (Sun et al., 1998). The granitic material represented a coarse-grained soil that has a relatively high saturated permeability ($k_{sat} = 3.5 \times 10^{-4}$ m/s), while the volcanic soil has a moderate saturated permeability of $6.9 \times 10^{-6}$ m/s. Figs. 2 and 3 show the soil water content curves (SWCC) and permeability matric suction functions of the soils (Sun et al., 1998).

### 3.2. Numerical model

Through analytical descriptions of all possible groundwater flow fields in infinite slope, Iverson (1990) shows that these flow fields may have any spatial orientation and may be affected by hydraulic anisotropy and heterogeneity, but they produce pore-water pressure and hydraulic gradients that vary only as functions of the space coordinate y, which is oriented normal to the slope (Figure 4) (Iverson, 1990, 2000). The results were supported by Lee et al. (2011) who compared the performances of two instrumented laboratory models, i.e. one-dimensional soil column and two-dimensional slope. They concluded that the simpler one-dimensional soil column can be used for the study of hydraulic response in single-layered homogeneous soil because the vertical flow plays a more dominant role than the lateral flow in this type of soil slope. For these reasons, one dimensional soil column model along *y*-direction was adopted in this numerical simulation.

The soil column model has the dimensions of 5 m in height, and 1 m in width (Figure 5). Fine quadrilateral elements ($0.5 \text{ m} \times 0.5 \text{ m}$) were used for the entire column. No flow boundary ($Q = 0$) was assigned at the bottom edge of the model representing the soil was underlain by an impermeable layer. For an infinite slope (such as that shown in

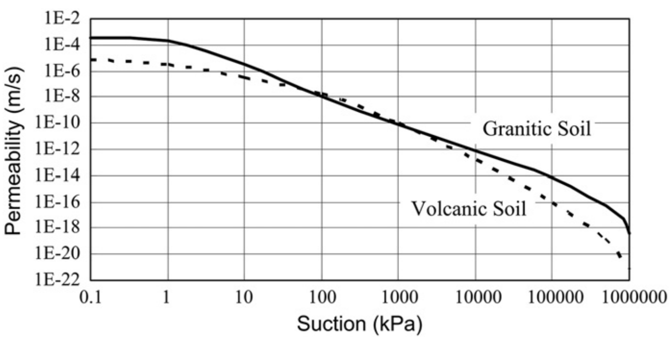


**Fig. 3.** Permeability functions for the completely weathered granitic material and the completely weathered volcanic material (Sun et al., 1998).

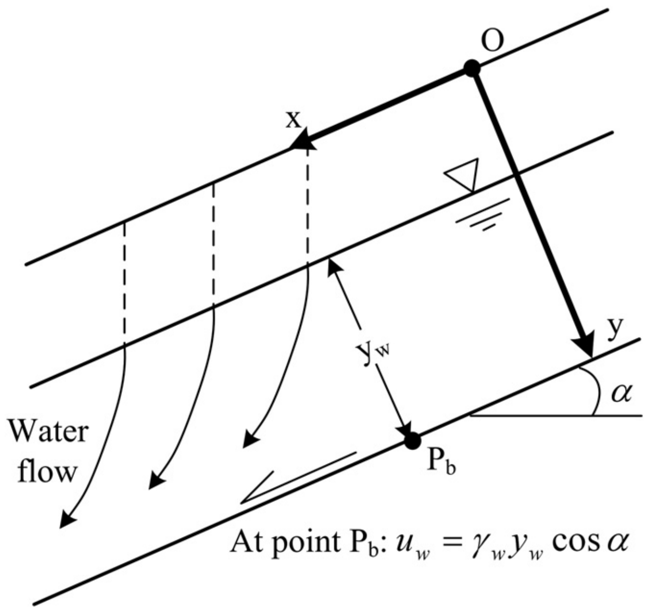


**Fig. 4.** Schematic illustrating the water flow in the infinite slope, which assumes no variation of any quantity in the *x* direction (modified from Iverson, 2000).

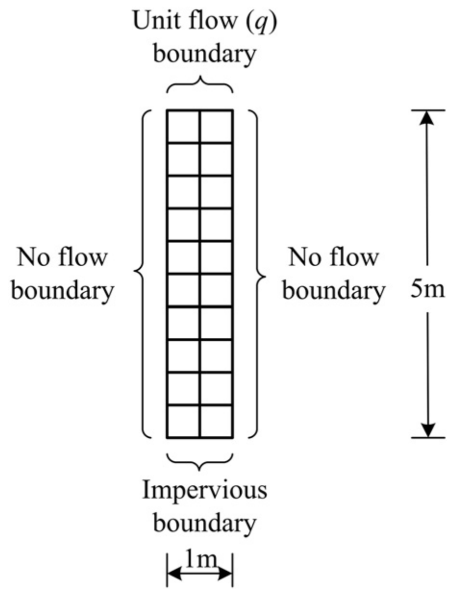


**Fig. 5.** One-dimensional soil column model.

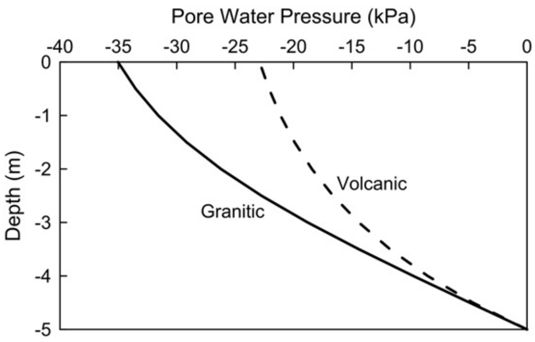


**Fig. 6.** Initial conditions for the numerical simulation.

Fig. 1), the direction of lateral flow is normally parallel with the underlying impermeable layer. The inflow to an arbitrary vertical column in the slope can be assumed to be equal to the outflow yielding a zero net influx into the column. Thus, the left and right edges of the soil column were also assigned as no flow boundaries ($Q=0$).

In this parametric study, three rainfall intensities, i.e. 5, 20 and 80 mm/h, were chosen to represent a low, a moderate, and an intense rainfall condition, respectively. The constant rainfalls were assigned as a unit flux boundary ($q$) with no ponding option on the top surface of the soil column. The no ponding option was adopted based on the rationale that the rainwater exceeding the infiltration capacity of soil will be drained away from the soil slope as surface runoff. The analysis was terminated once the water table has risen to the column surface.

The initial condition, which was required for performing the transient infiltration analysis, was obtained by running a steady-state analysis with a so-called background rainfall intensity of 10 mm/day. Fig. 6 shows the initial conditions corresponding to the volcanic and granitic soils. These profiles generally resembled those obtained from field measurements (Sun et al., 1998).

### 3.3. Simulation results

Figs. 7 and 8 present the vertical pore-water pressure profiles for the granitic soil and volcanic soil, respectively, under the three constant rainfall intensities, while Figs. 9 and 10 show the variations of pore-water pressure over time for the two soils, respectively. From the pore-water pressure results, it can be concluded that the hydraulic responses of soils to rainfall can essentially be divided into two main stages:

(1) The first stage is a process involving propagation of wetting front until it reaches the interface of impermeable layer (Figures 9 and 10). In this stage, the variations in matric suction are predominant. When rainfall intensity is lower than the saturated permeability of soil (i.e. $I<k_{sat}$ or $I/k_{sat}<1$), the matric suction decreases significantly due to the propagation of wetting front. Nevertheless, the soil still remains in the unsaturated state as the matric suction behind the wetting front is not completely dissipated. Figs. 7 and 8a and b show that the higher the ratio of rainfall intensity to saturated permeability of soil ($I/k_{sat}$), the lower the matric suction behind the wetting front. These observations showed good agreements with the experimental findings reported by Lee et al. (2011). When rainfall intensity is higher than the saturated permeability of soil (i.e. $I>k_{sat}$ or $I/k_{sat}>1$), the matric suction will be wholly dissipated during the propagation of wetting front, as shown in Fig. 8c.

(2) The second stage involves rise of water table which occurs instantly after the first stage (Figures 9 and 10). In this stage, the increase of positive hydrostatic pore-water pressure is predominant. The mechanism of the rise of water table can be observed

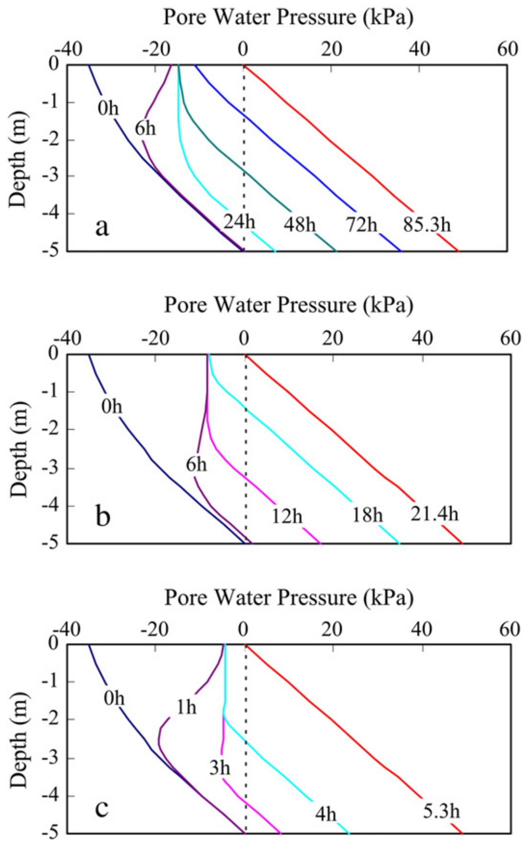


**Fig. 7.** Vertical transient pore-water pressure profiles for the granitic soil under constant rainfall intensities: (a) 5 mm/h ($I/k_{sat}=0.004$); (b) 20 mm/h ($I/k_{sat}=0.016$); (c) 80 mm/h ($I/k_{sat}=0.063$).

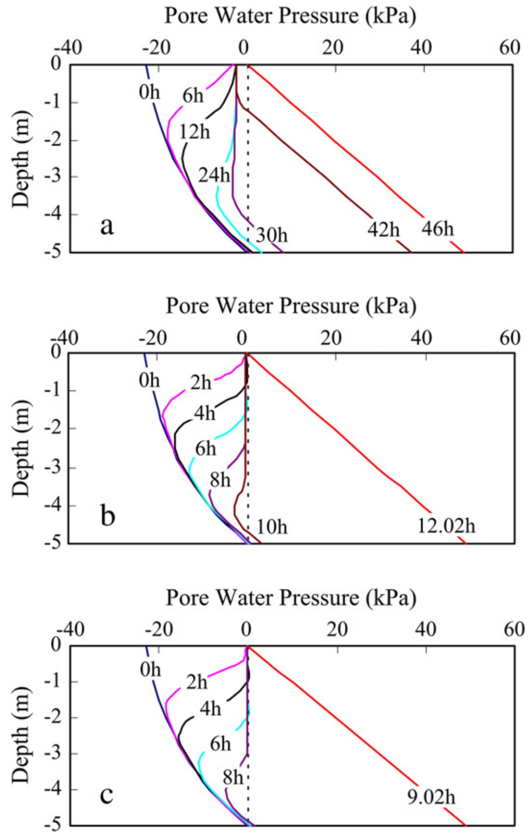


**Fig. 8.** Vertical transient pore-water pressure profiles for the volcanic soil under constant rainfall intensities: (a) 5 mm/h ($I/k_{sat}=0.2$); (b) 20 mm/h ($I/k_{sat}=0.8$); (c) 80 mm/h ($I/k_{sat}=3.2$).

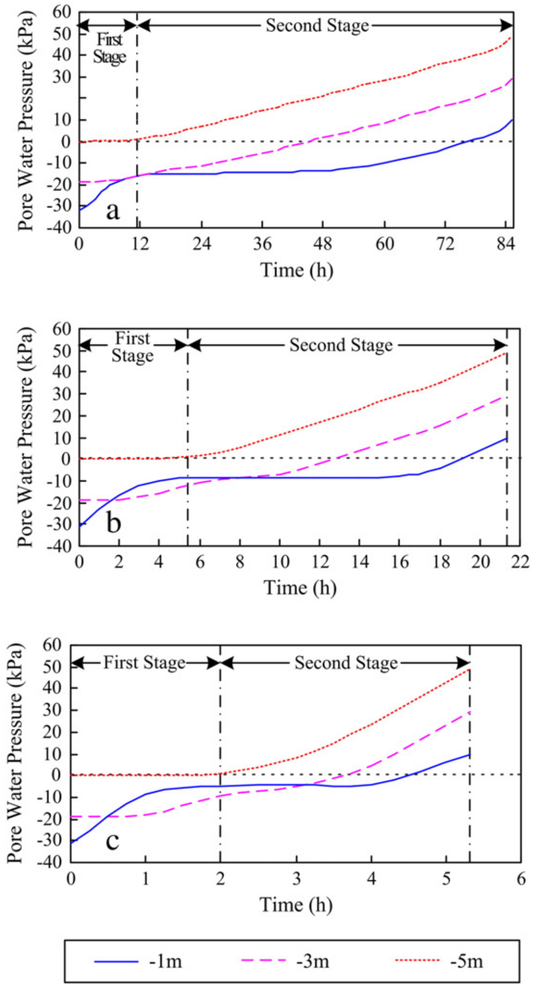


**Fig. 9.** Variations of pore-water pressures over time for the granitic soil under constant rainfall intensities: (a) 5 mm/h ($I/k_{sat}=0.004$); (b) 20 mm/h ($I/k_{sat}=0.016$); (c) 80 mm/h ($I/k_{sat}=0.063$).

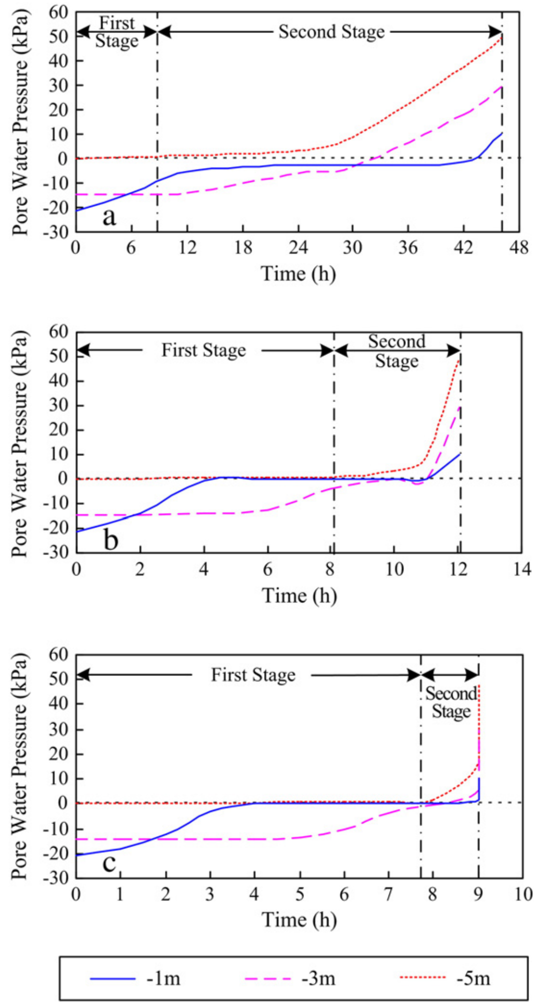


**Fig. 10.** Variations of pore-water pressures over time for the volcanic soil under constant rainfall intensities: (a) 5 mm/h ($I/k_{sat}=0.2$); (b) 20 mm/h ($I/k_{sat}=0.8$); (c) 80 mm/h ($I/k_{sat}=3.2$).

through the positive pore-water pressure developed at the interface of the impermeable layer at −5 m elevation, as indicated by the red dotted lines in Figs. 9 and 10. The rate of rise of the water table is strongly affected by the rainfall intensity and saturated permeability of soil. Within a same soil, when the rainfall intensity is lower than the saturated permeability (i.e. $I<k_{sat}$ or $I/k_{sat}<1$), the rate of rise of the water table increases with an increase in $I/k_{sat}$ ratio. When the $I/k_{sat}$ ratio exceeds unity, the water table rises almost instantaneously, as shown in Fig. 10c. Similar observations were obtained from the field experiments carried out by Springman (2010) and Askarinejad et al. (2010). By comparing the rise of water table in Figs. 9 and 10, it is found that the findings above are only valid within a same type of soil. There is no continual trend between the two types of soil. The results imply that besides the rainfall intensity and saturated permeability of soil, other hydraulic properties of soil such as SWCC and permeability matric suction function could also play a role in the mechanism of rise of water table.

## 4. Influence of hydraulic responses on surficial failures

To clarify the influence of hydraulic responses of soil on the mechanism of surficial slope failure, Eq. (6) can be simplified as:

$$\mathrm{FOS} = A + \frac{B}{z_w} \tag{7}$$

where

$$A = \frac{\tan\theta'}{\tan\alpha}$$

$$B = \frac{c' - \sigma^s \tan\theta'}{\gamma_t \sin\alpha\cos\alpha}$$

The component $A$ in Eq. (7) is a function of slope angle ($\alpha$) and soil internal friction angle ($\phi'$). These parameters are regarded as contributing factors to slope stability which are unaffected by the hydraulic responses of soil. On the contrary, the component $B$ consists of the suction stress characteristic curve ($\sigma^s$) which is a variable subject to the hydraulic responses of soil to rainfall.

### 4.1. Surficial failure induced by propagation of wetting front

In the first stage of hydraulic responses, the propagation of wetting front caused a reduction in matric suction, with no positive hydrostatic pore-water pressure generated. Under such circumstances, it is safe to say that the component $B$ in Eq. (7) will never become negative, and the component $A$ appears to be the limiting value for the factor of safety of slope. For a slope that has a soil internal friction angle ($\phi'$) greater than slope angle ($\alpha$), i.e. $A>1$, the slope will remain stable throughout the propagation of wetting front (Figure 11b). Conversely, if $A<1$, slope failure induced by the loss of matric suction is possible. The depth of failure plane ($z_f$) can be deduced from Eq. (6) by taking FOS equal to unity:

$$z_f = \frac{c' - \sigma^s \tan\theta'}{\gamma_t \cos^2\alpha(\tan\alpha - \tan\theta')} \quad (8)$$

Eq. (8) can be rewritten as follows:

$$z_f = C - D\sigma^s \quad (9)$$

where

$$C = \frac{c'}{\gamma_t \cos^2\alpha(\tan\alpha - \tan\theta')}$$

$$D = \frac{\tan\theta'}{\gamma_t \cos^2\alpha(\tan\alpha - \tan\theta')}$$

For an existing slope in which the c', ϕ', and $\alpha$ parameters are assumed to remain unchanged throughout the infiltration process, the components C and D can thus be treated as constants. The linear relationship of Eq. (9) can be presented graphically in Fig. 12.

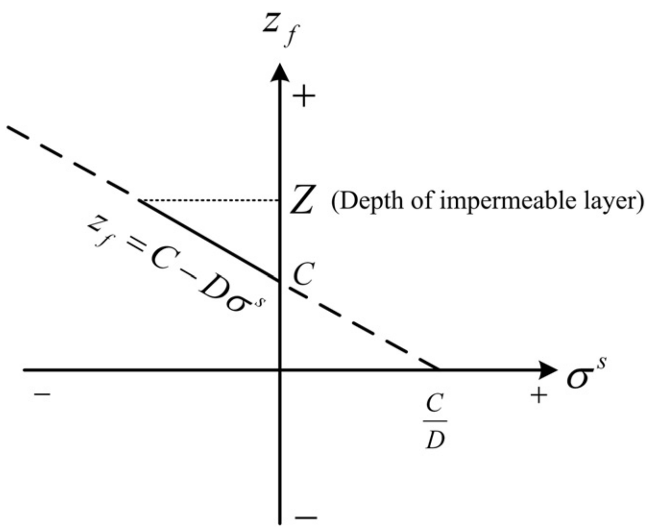


**Fig. 12.** Relationship between depth of failure plane and suction stress characteristic curve ($\sigma^s$).

From Fig. 12, it is obvious that the possible depth of failure plane caused by the propagation of wetting front is in between Z and C, where Z is the depth from ground surface to impermeable layer (Figure 1). The depth of failure plane is controlled linearly by the suction stress characteristic curve ($\sigma^S$) which in turn is characterized by the degree of saturation ($S_e$) and matric suction ($u_w$). Within the zone of wetting front, the soil is normally close to full saturation; thus, $S_e$ can be reasonably assumed to be equal to unity. As the result, the depth of failure plane is solely dictated by the matric suction behind the wetting front. The lower the matric suction, the shallower the failure plane of the slope. The shallowest failure plane occurs when matric suction is completely dissipated. This is associated with the condition of $I/k_{sat} > 1$, as demonstrated in Fig. 8c. The shallowest failure plane is equal to C, which is a function of the effective cohesion of soil. This explains the failures of cohensionless soil slopes tend to be shallow during intense rainfall.

If the computed depth of failure plane ($z_f$) is greater than the thickness of soil concerned (Z), the slope failure induced by the propagation of wetting front is unlikely to occur. Under this condition, the slope failure could be triggered by the rise of water table (stage two of hydraulic response) which will be discussed in the following section.

### 4.2. Surficial failure induced by rise of water table

The instability of slope due to the rise of water table (stage 2 of hydraulic response) should be assessed if the slope still remains stable after the propagation of wetting front (stage 1 of hydraulic response). In this stage, the positive hydrostatic pore-water pressure increases with the rise of water table. Similarly, the FOS of the slope can be calculated by making reference to Eq. (7). As the highest positive pore-water pressure always occurs on the interface of impermeable layer, as indicated in Figs. 7 and 8, this would certainly yield the highest suction stress characteristic curve ($\sigma^s$), and the lowest B component and FOS.

Fig. 13a depicts the relationships between variations in FOS and depth of failure plane. During the propagation of wetting front, the FOS decreases gradually from point N to point O with the increase in depth of failure plane. The FOS at point O is controlled by the limiting value of component A, as explained in Section 4.1. The development of positive pore-water pressure at the interface of impermeable layer is a prerequisite to further reduce the FOS from point O to the critical FOS value of 1 (point P). The FOS may drop from point O to point P following different paths subjects to the intensity of rainfall (Figure 13b). A low intensity rainfall would results in a slow reduction of FOS (Path O′–P′). This can be explained by the variations of pore-water pressures shown in Fig. 10a. The increase of positive pore-water pressure from 0 to 50 kPa requires a continuous rainfall of more than 35 h. On the contrary, a sudden drop of FOS (Path O′– P″) can be expected when an intense rainfall is applied on the slope. The intense rainfall has caused the pore water pressures at the interface of impermeable layer increased instantaneously (within 2 h) after the stage one of hydraulic response (Figure 10c). These observations reveal that slopes are prone to sudden failure under intense rainfall condition.

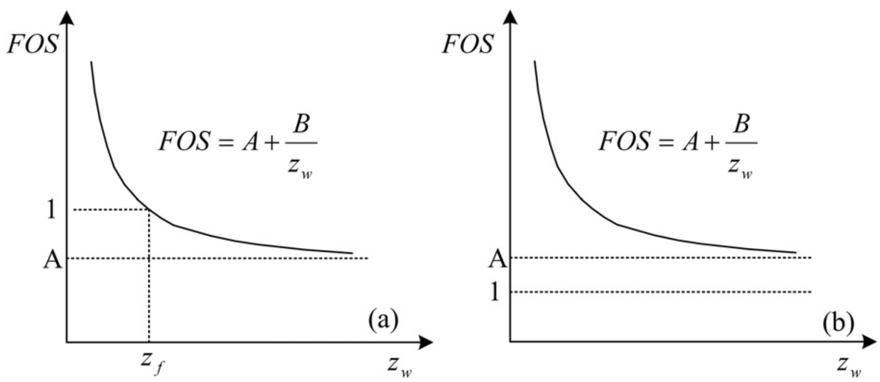


**Fig. 11.** Relationships between factor of safety and propagation of wetting front for: (a) $A<1$; (b) $A>1$.

## 5. Discussions

### 5.1. Effective stress under unsaturated conditions

The limit equilibrium factor of safety equation in this study was developed based on the relatively new unified concept of effective stress as proposed by Lu and Likos (2006) and Lu and Godt (2008). The validities of the findings are further verified by adopting the more widely accepted independent stress state variable approach as proposed by Fredlund et al. (1978). In this approach, the shear strength contributions from the net normal stress and matric suction are characterized by the soil internal friction angle ($\phi'$) and the angle of frictional resistance due to the contribution of matric suction ($\phi^b$):

$$\tau_f = c' + (\sigma_n - u_a)\tan\theta' + (u_a - u_w)\tan\theta^b \tag{10}$$

The limit equilibrium factor of safety equation can then be expressed as (Cho and Lee, 2002):

$$\mathrm{FOS} = \frac{c' + (\sigma_n - u_a)\tan\theta' + (u_a - u_w)\tan\theta^b}{\gamma_t z_w \sin\alpha\cos\alpha} \tag{11}$$

Fredlund et al. (1996) found that $\phi^b$ remains constant and can be approximated to $\phi'$ up to the air entry value (AEV) of soil. Beyond the AEV, $\phi^b$ decreases to 1/2–2/3 of $\phi'$. During the propagation of wetting front, the matric suction behind the wetting front is very likely to be below the AEV. Thus, the $\phi^b$ can be conveniently taken as equal to $\phi'$. With this assumption, Eq. (11) can be simplified as:

$$\mathrm{FOS} = \frac{c' + \left(\gamma_t z_w \cos^2\alpha - u_w\right)\tan\theta'}{\gamma_t z_w \sin\alpha\cos\alpha} \tag{12}$$

The expressions in Eq. (12) developed from the independent stress state variable approach (Fredlund et al., 1978) were found to be analogous to Eq. (6) developed from the unified stress approach (Lu and Likos, 2006; Lu and Godt, 2008). It appears that Eq. (12) is just referring to a specific condition of unsaturated soil (when the soil close to full saturation and matric suction is below AEV), while Eq. (6) can be applied universally for the soils in both partially or wholly saturated conditions. This proves that the findings in this study are valid regardless of which stress approach is adopted in developing the model.

### 5.2. 1-Dimensional versus 2-dimensional analyses

Fig. 10c shows that water table rises almost instantaneously when $I/k_{sat}$ ratio exceeds unity. Since the one-dimensional model simulated in the present study has neglected lateral flow effect, the validity of the instantaneous water table rise phenomenon observed may be questionable. A more rigorous two-dimensional model was adopted to further verify the observation. The two-dimensional model was constructed at a typical slope angle of 25°, vertical height of 5 m, and horizontal length of 60 m, as illustrated in Fig. 14. For an indisputable comparison to the result of Fig. 10c, the two-dimensional model was assigned with the hydraulic properties of volcanic soil. Rainfall intensity of 80 mm/h was applied to the top boundary, while the side and bottom boundary conditions were identical to that of one-dimensional model.

To eliminate the influence of side boundary of two-dimensional model on the hydraulic responses, only the pore-water pressure on the interface of impermeable layer at the middle slope was selected for comparison purpose. Fig. 15 shows the comparison results of pore-water pressures between the one and two-dimensional models. The patterns of pore-water pressure variations for the two models were found to be comparable, in which the water table increased almost instantaneously after certain elapsed time. However, it should be noted that the hydraulic response of the two-dimensional model (11.7 h) was slower than that of the one-dimensional model (9 h). Besides, the ultimate pore water pressure of the two-dimensional model (40.3 kPa) was also lower than that of the one-dimensional model (49.0 kPa). These observations can be attributed to the influence of slope angle on hydraulic gradient and gravity component, as well as the lateral flow effect. From the foregoing comparison, it can be concluded that the instantaneous water table rise when $I/k_{sat}$ ratio exceeds unity observed in the one-dimensional model may represent a real phenomenon occurs in an infinite slope.

### 5.3. Hydraulic response and slope stability to rainfall infiltration

This study provided an insight into the hydraulic responses of soil to various rainfall characteristics and soil permeability, and related these hydraulic responses to the type and mechanism of slope failures. From the numerical and analytical analyses, some simple yet useful equations and figures were reported for anticipating the type and mechanism of surficial slope failures.

The hydraulic responses of soil slope to rainfall infiltration can essentially be divided into two stages, namely, propagation of wetting front, and rise of water table. For a slope with the soil internal friction angle ($\phi'$) greater than slope angle ($\alpha$), the slope will never fail through propagation of wetting front. The development of positive pore-water pressure induced by the rise of water table is required to trigger the failure. The failure plane for this type of failure is normally developed on the interface of impermeable layer where the positive pore-water pressure is the highest.

For a slope with the soil internal friction angle ($\phi'$) smaller than slope angle ($\alpha$), the slope failure is potentially induced by the propagation of wetting front provided the thickness of soil above the impermeable layer is sufficient for the development of failure plane. This type of failure mechanism would normally require a rainfall of relatively shorter duration compared to the case of rise of water table. The depth of failure plane is influenced by the matric suction behind the wetting front, which

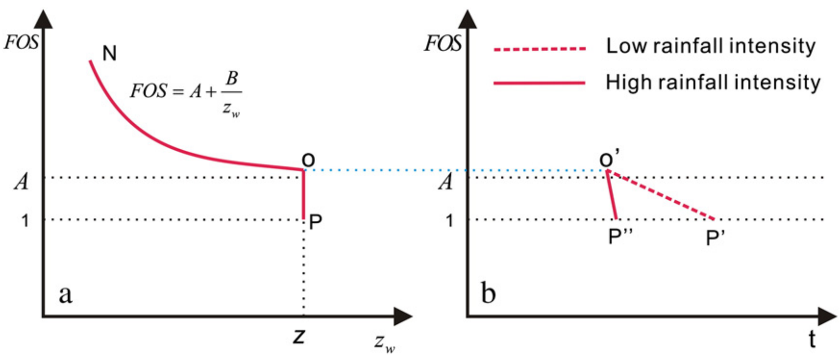


**Fig. 13.** Relationships between factor of safety due to rise of water table and: (a) depth of failure plane; (b) time of occurrence.

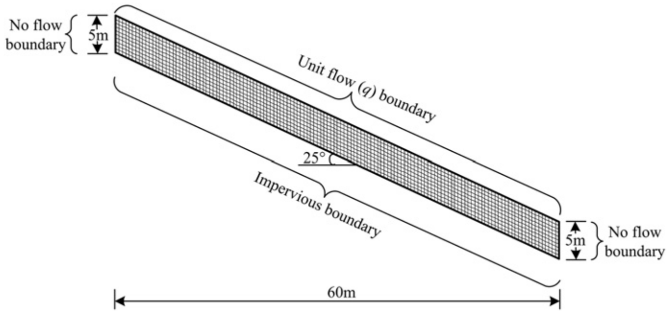


**Fig. 14.** Two-dimensional slope model.

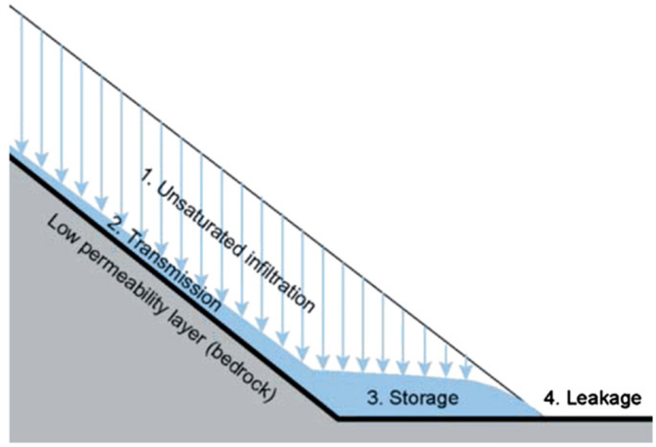


**Fig. 16.** Accumulation of rainwater at the toe of finite slope due to lateral flow (reproduced from Take et al., 2004).

in turn is governed by the rainfall intensity. An intense rainfall would result in a low matric suction behind the wetting front, and hence a shallow failure plane.

Besides the rainfall intensity, Ng and Shi (1998) found that the factor of safety of slope is also influenced by the rainfall duration. In reality, the intense rainfall is normally characterized by short duration. The short duration rainfall may not be sufficient to induce the rise of water table (stage 2 of hydraulic responses). Thus, a shallow failure induced by the propagation of wetting front is a more probable type of failure under this rainfall condition. On the contrary, the low intensity rainfall is normally of long duration. The potential slope failure plane for this type of rainfall is relatively deep due to the presence of matric suction behind the wetting front. The failure plane will be ultimately developed along the interface of impermeable layer if the rainfall duration is sufficiently long to induce a rise of water table.

The findings reported in this study were developed based on an infinite slope model. The infinite model made it simpler and more attractive in describing the failure initiation of slope. Somehow, the use of this simplified model has imposed certain limitations on the practical applications of the findings. This is because the actual slope is normally more realistically represented by a finite model. In the finite slope model, the lateral flow, which is neglected in this infinite model, could be predominant. This would result in an accumulation of water at the toe of slope fomented by the emergence of lateral flow, as shown in Fig. 16 (Take et al., 2004). Furthermore, the infinite model considered in this study constitutes a homogeneous soil layer underlain by an impermeable layer (bedrock). In reality, the soil profile may be characterized by two or more layers of soils overlying the bedrock. As the hydraulic responses of overlying soil are significantly governed by the hydraulic properties of the underlying soil, this area is worthy of further investigations.

## 6. Conclusions

A series of numerical simulations were carried out to investigate the hydraulic responses of soil to various rainfall characteristics and saturated permeability. The findings from the numerical simulations were used to explain analytically the type and mechanism of surficial slope failures. The following conclusions can be drawn from this study:

(1) The hydraulic responses to rainfall for a homogeneous infinite slope underlain by an impermeable layer can be divided into two stages. The first stage involves the propagation of wetting front, while the second stage constitutes the rise of water table. The rainfall intensity and saturated permeability control the two stages of hydraulic responses. In the first stage, the higher the rainfall intensity, the lower the matric suction behind the wetting front. The matric suction is wholly dissipated if the rainfall intensity is higher than the saturated permeability of soil. In the second stage, the higher the rainfall intensity, the quicker the rise of water table. The water table rises almost instantaneously if the rainfall intensity is higher than the saturated permeability of soil.

(2) The type and failure mechanism of a slope are controlled by the hydraulic responses of soil to rainfall, which in turn are governed by the combined effects of rainfall intensity and saturated permeability. In the first stage of hydraulic response, both the rainfall intensity and saturated permeability control the depth of failure plane of slope through the propagation of wetting front. The higher the ratio of rainfall intensity to saturated permeability of soil, the shallower the failure plane of the slope. In the second stage of hydraulic response, both the rainfall intensity and saturated permeability control the occurrence time of failure. When the rainfall intensity is higher than the saturated permeability of soil, positive pore-water pressures may develop instantaneously on the interface of impermeable layer resulting in sudden drops of shear resistance and factor of safety.

(3) The contributing factors of slope such as soil internal friction angle ($\phi'$) and slope angle ($\alpha$) could also influence the mechanism of surficial slope failure. For a slope with the soil internal friction angle ($\phi'$) greater than slope angle ($\alpha$), the slope will never fail through loss of matric suction during the propagation of wetting front. This type of slope is more likely to be associated with the failure mechanism induced by the rise of water table. On the contrary, the slope with the soil internal friction angle ($\phi'$) lower than slope angle ($\alpha$) is likely to be triggered by the propagation of wetting front if sufficient thickness of soil exists above the impermeable layer for the development of failure plane.

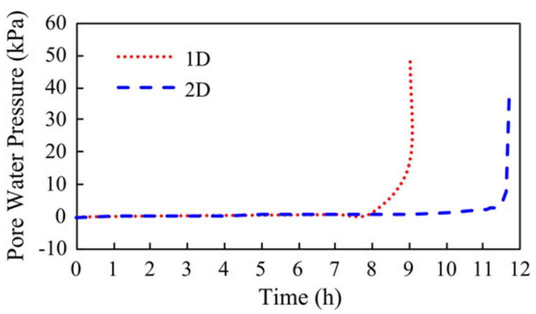


**Fig. 15.** Comparing of variations of pore-water pressures at the interface of the impermeable layer for the volcanic soil under constant rainfall intensities 80 mm/h ($I/k_{sat} = 3.2$).

## Acknowledgments

The authors would like to acknowledge the financial supports from National Program on Key Basic Research Project (973 Program, 2013CB036400) and National Natural Science Foundation of China for Youth (No. 51004065).

## References


Aitchison, G.D., 1960. Relationships of moisture stress and effective stress functions in unsaturated soils. In: Proceedings of the conference on Pore Pressure and Suction in Soils. Butterworths, London, UK, pp. 47–52.

Aleotti, P., 2004. A warning system for rainfall-induced shallow failures. Engineering Geology 73, 247–265.

Apip, K., Takara, K., Yamashiki, Y., Ibrahim, A.B., 2009. Study on early warning system for shallow lanslides in the upper Citarum River catchment, Indonesia. Annuals of Disaster Prevention Research Institute, Kyoto University, Japan, 52B, pp. 9–17.

Askarinejad, A., Casini, F., Kienzler, P., Teysseire, P., Springman, S.M., 2010. Mountain risks: two case histories of landslides induced by artificial rainfall on steep slopes. International Conference of 'Mountain Risks: Bringing Science to Society', pp. 201–206 (Florence, Italy).

Au, S., 1998. Rain-induced slope instability in Hong Kong. Engineering Geology 51 (1), 1–36.

Bishop, A.W., 1959. The Principle of Effective Stress. Norwegian Geotechnical Institute, Oslo, Norway.

Cardinali, M., Galli, M., Guzzetti, F., Ardizzone, F., Reichenbach, P., Bartoccini, P., 2006. Rainfall induced landslides in December 2004 in south-western Umbria, central Italy: types, extent, damage and risk assessment. Natural Hazards and Earth System Sciences 6, 237–260.

Chigira, M., Nakamoto, M., Nakata, E., 2002. Weathering mechanisms and their effects on the landsliding of ignimbrite subject to vapor-phase crystallization in the Shirakawa pyroclastic flow, northern Japan. Engineering Geology 66, 111–125.

Cho, S.E., Lee, S.R., 2001. Instability of unsaturated soil slopes due to infiltration. Computers and Geotechnics 28 (3), 185–208.

Cho, S.E., Lee, S.R., 2002. Evaluation of surficial stability for homogeneous slopes considering rainfall characteristics. Journal of Geotechnical and Geoenvironmental Engineering 128, 756–763.

Collins, B.D., Znidarcic, D., 2004. Stability analyses of rainfall induced landslides. Journal of Geotechnical and Geoenvironmental Engineering, ASCE 130 (4), 362–372.

Crosta, G.B., Frattini, P., 2003. Distributed modeling of shallow landslides triggered by intense rainfall. Natural Hazards and Earth System Sciences 3, 81–93.

Dai, F., Lee, C., et al., 1999. Analysis of rainstorm-induced slide-debris flows on natural terrain of Lantau Island, Hong Kong. Engineering Geology 51 (4), 279–290.

De Vita, P., Napolitano, E., Godt, J., Baum, R., 2012. Deterministic estimation of hydrological thresholds for shallow landslide initiation and slope stability models—Case study from the Somma-Vesuvius area of southern Italy. Landslides. http://dx.doi.org/10.1007/s10346-012-0348-2.

Fredlund, D.G., Morgenstern, N.R., Widger, R.A., 1978. The shear strength of unsaturated soil. Canadian Geotechical Journal 15, 313–321.

Fredlund, D.G., Xing, A., Fredlund, M.D., Barbour, S.L., 1996. The relationship of the unsaturated soil shear strength to the soil water characteristic curve. Canadian Geotechnical Journal 32, 440–448.

GeoSlope International Ltd., 2007. Seep/W user's guide for finite element seepage analysis. GEO-SLOPE International Ltd., Calgary, Alta.

Godt, J.W., Baum, R.L., Lu, N., 2009. Landslideing in partially saturated materials. Geophysical Research Letters 36, L02403.

Godt, J.W., Şener-Kaya, B., Lu, N., Baum, R.L., 2012. Stability of infinite slopes under transient partially saturated seepage conditions. Water Resources Research 48, W05505. http://dx.doi.org/10.1029/2011WR011408.

Guzzeti, F., Peruccacci, S., Rossi, M., Stark, C.P., 2008. The rainfall intensity-duration control of shallow landslides and debris flows: an update. Landslides 5, 3–17.

Iverson, R.M., 1990. Groundwater flow fields in infinite slopes. Geotechnique 40 (1), 139–143.

Iverson, R.M., 2000. Landslide triggering by rain infiltration. Water Resources Research 36 (7), 1897–1910.

Jennings, J.E., Burland, J.B., 1962. Limitations to the use of effective stresses in partly saturated soils. Geotechnique 12 (2), 125–144.

Kasim, F., Fredlund, D.G., Gan, J.K.M., 1998. Effect of steady state rainfall on long term matric suction conditions in slopes. Proceedings, 2nd Int. Conf. on Unsaturated Soils, pp. 78–83 (Beijing, China).

Keefer, D.K., Wilson, R.C., Mark, R.K., et al., 1987. Real-time landslide warning during heavy rainfall. Science 238, 921–925.

Lee, L.M., Gofar, N., Rahardjo, H., 2009. A simple model for preliminary evaluation of rainfall-induced slope instability. Engineering Geology 108, 272–285.

Lee, L.M., Kassim, A., Gofar, N., 2011. Performances of two instrumented laboratory models for the study of rainfall infiltration into unsaturated soils. Engineering Geology 117, 78–89.

Leroueil, S., 2001. Natural slopes and cuts: movement and failure mechanisms. Geotechnique 51 (3), 197–243.

Lu, N., Godt, J., 2008. Infinite slope stability under steady unsaturated seepage conditions. Water Resources Research 44, W11404.

Lu, N., Likos, W.J., 2006. Suction stress characteristic curve for unsaturated soil. Journal of Geotechnical and Geoenvironmental Engineering 132, 131–142.

Mein, R.G., Larson, C.L., 1973. Modeling infiltration during a steady rain. Water Resources Research 9 (2), 384–394.

Ng, C.W.W., Shi, Q., 1998. Influence of rainfall intensity and duration on slope stability in unsaturated soils. Quarterly Journal of Engineering Geology & Hydrogeology 31 (2), 105–113.

Ng, C.W.W., Chen, S.Y., Pang, Y.W., 1999. Parametric study of the effects of rain infiltration on unsaturated slopes. Rock Soil Mechanics 20 (1), 1–14.

Ng, C.W.W., Wang, B., Tung, Y.K., 2001. Three-dimensional numerical investigations of groundwater responses in an unsaturated slope subjected to various rainfall patterns. Canadian Geotechnical Journal 38, 1049–1062.

Pradel, D., Raad, G., 1993. Effect of permeability on surficial stability of homogeneous slopes. Journal of Geotechnical Engineering 119 (2), 315–332.

Rahardjo, H., Ong, T.H., Rezaur, R.B., Leong, E.C., 2007. Factors controlling instability of homogeneous soil slopes under rainfall. Journal of Geotechnical and Geoenvironmental Engineering 133 (12), 1532–1543.

Rahardjo, H., Rezaur, R.B., Leong, E.C., 2009. Mechanism of rainfall-induced slope failures in tropical regions. The 1st Italian Workshop on Landslides. Napoli, Italy, 8 – 10 June 2009.

Skempton, A., DeLory, F., 1957. Stability of natural slopes in London Clay. Proc. 4th Int. Conf. Soil Mech. Found. Engrg.

Soddu, S., Delitala, G., Sciabica, M., Barrocu, G., 2003. Modelling groundwater effects on slope stability. Materials and Geoenvironmental 50 (1), 349–352.

Springman, S., 2010. The Rüdlingen Experiment - Landslide triggering by artificial rainfall: hydrological aspects. Synthesis report of research project TRAMM, pp. 22–23.

Sun, H.W., Wong, H.N., Ho, K.K.S., 1998. Analysis of infiltration in unsaturated ground. Proc. Annual Seminar on Slope Engineering in Hong Kong. Balkema Publisher, Hong Kong.

Take, W., Bolton, M., Wong, P., Yeung, F., 2004. Evaluation of landslide triggering mechanisms in model fill slopes. Landslides 1 (3), 173–184.

Terzaghi, K., 1936. The shearing resistance of saturated soils. Proc., 1st Int. Conf. on Soil Mechanics, vol. 1. Cambridge, Mass., pp. 54–56.

Toll, D., 2001. Rainfaill-induced landslides in Singapore. Proceedings of the Institution of Civil Engineers-Geotechnical Engineering 149 (4), 211–216.

Wieczorek, G.F., 1987. Effect of rainfall intensity and duration on debris flows in central Santa Cruz Mountains, California. Geological Society of America Reviews in Engineering Geology 7, 93–104.